

## Research Article

# Nutritional Analysis of *Elote Tamales* Cooked in a Hybrid-Solar Cooker

J. A. del Río , Arnold A. Hernández-Medina , and Anabel López-Ortiz 

*Instituto de Energías Renovables, Universidad Nacional Autónoma de México, Priv. Xochicalco s/n, Temixco, 62580 Morelos, Mexico*

Correspondence should be addressed to Anabel López-Ortiz; alo@ier.unam.mx

Received 9 December 2022; Revised 31 August 2023; Accepted 19 September 2023; Published 12 October 2023

Academic Editor: Ali Ganjloo

Copyright © 2023 J. A. del Río et al. This is an open access article distributed under the Creative Commons Attribution License, which permits unrestricted use, distribution, and reproduction in any medium, provided the original work is properly cited.

Cooking traditional meals using a solar cooker is often challenging because it may require maintaining temperatures of 63 to 180°C for extended periods. A popular Mesoamerican/Mexican dish, “tamale,” is a vapor-cooked corn dough meal/flour wrapped inside corn husk, which may be prepared in a solar cooker. However, its nutritionally rich variety, “elote tamal” prepared from ground fresh corn kernels of tender corncobs with added sugar, fresh milk, and butter, becomes unpalatable under such solar cooking. The initial slow rise in temperature leads to the fermentation of the dough-milk mix and degrades the product. We show that an auxiliary electric heater boosting the temperature at the initial period in an electric-solar hybrid cooker can overcome this limitation. Furthermore, we found significant differences in the total sugar and titratable acidity in the slow-cooked *elote tamal*. These differences are associated with the incipient fermentation introduced in the milk-containing dough mix during the slow heating stage in traditional solar cooking. We analyzed and compared the protein, fat, moisture content, ash, total sugars, total fibers, titratable acidity, and color of *elote tamales* prepared under four different cooking conditions. Milk-based tamales under solar cooking require an additional thermal booster at the initial stage to avoid fermentation and eventual loss of quality of the cooked dish. This research is also relevant to the solar cooking of other milk-based meals.

## 1. Practical Applications

The solar cooker device was designed considering the possibility of cooking any day, including cloud days. The solar cooking time is longer than conventional cooking, but the time preparation is shorter than traditional. The sensory perception for solar meals is similar to traditional cooking ones and demonstrates the same nutritional characteristics as conventional cooking. Therefore, our results show that a solar cooking device reaches similar characteristics to the food product obtained from the traditional cooking process. However, our results alert us about the solar cooking of meals containing milk or any other ingredient with fermentation possibility. In this case, the cooking procedure needs to be faster. Also, our results encourage the transition to solar cooking, persuading the environmental and general health benefits of solar cooking.

## 2. Introduction

Worldwide, gastronomy is an intangible aspect of civilization, closely related to our culture. Traditional Mexican cuisine was declared *Intangible Heritage of Humanity* by the United Nations Educational, Scientific and Cultural Organization [1]. In particular, the traditional dishes involving maize (corn) subjected to the nixtamalization process (NIX) are noteworthy. This process involves lime-hulling the maize, which increases its nutritional value. The present work relates to tamal (Tamales originates from tamalii, the Aztec-Mexican word for wrapped food; elote–corn-cob) (pronounced, *tamal*) that is a traditional Mesoamerican dish, usually made from the corn-based dough (with or without the NIX process) folded in a cornhusk (the leaf-like permeable sheath covering the corncob) or banana leaf and steamed. It forms part of everyday Mexican cuisine,

with many modified versions available on festive occasions, depending on the region.

Depending on the variety, a tamal may be of 100–200 g wet mass, with a calorific value of 150–300 kilocalories (Cal), fat (45%), carbohydrates (45%), and protein (10%) with appreciable recommended daily allowance (RDA) of dietary fiber, calcium, iron, and potassium [2].

Nevertheless, food composition may change due to preparation methods, cooking procedures, and technologies. Mariscal-Moreno et al. [3] test different preparation methods (traditional NIX: 1% calcium hydroxide, ecological NIX: 1% calcium carbonate, 1% wood ash as lime, without salt (without NIX)). They found different results for calcium carbonate treatment (protein  $7.1 \pm 0.4\%$ ; fat  $20.6 \pm 0.3\%$ ; ash  $6.21 \pm 0.01$ ; total dietary fiber  $6.9 \pm 0.3\%$ ; total starch  $47.6 \pm 0.3\%$ ). They found significant fiber concentration and lower values in starch content with carbonate treatment. Guzmán et al. [4] found different protein compositions in tamales due to the cooking time and alkalization process. In this work, the preparation was without the NIX process and with raw elote-corn cob.

Traditionally, *tamal* dishes are prepared by stacking the wrapped dough mix on a base of twigs inside large vessels, with water contained at the bottom and boiled using firewood. However, the massive use of wood stoves leads to forest degradation/deforestation and greenhouse gas emissions. They can also seriously impact the health of rural populations [5–8]. Although wood's annual fuel cost is cheaper (almost free) than gas or electricity in some regions [9], it is not environmentally friendly in large-scale and sustained use. Thus, efficient low-emission cooking technologies require attention. Solar cookers have been proposed as an alternative. The use of solar cookers helps eliminate high concentrations of particulate matter in the cooking ambient, the inhalation of which is harmful to humans [10]. Since the first solar cooker was developed in India in 1878 [11], researchers have been trying to improve their efficiency [12], including geometrical features [9, 13, 14], maximum temperature attained [15, 16], energetic cost reduction [17, 18], CO<sub>2</sub> emission reduction [19, 20], among their many other attributes [9, 21, 22].

There are different types of solar cookers, which can be classified according to their heat transfer mechanism [23]:

- (i) Direct solar cookers use solar energy directly to heat the cooking chamber
- (ii) Indirect solar cookers heat the chamber using a fluid (water, oil, air, etc.) heated by solar energy
- (iii) Mixed solar cookers use more than one solar/renewable energy technology, and
- (iv) Hybrid solar cookers use both renewable and non-renewable energy sources

Also, in the literature, we can find different designs, which include small hollow copper-made balls used to improve heat transfer, an aluminum-made trapezoidal duct with a 200 W halogen lamp placed inside to enhance the

heat transfer, and a 10 W fan; the best configuration was with solar energy only, using the small hollow balls [24]. In other paper, authors also tried different sensible heat storage materials (blackened pebbles, masonry bricks, and aluminum balls). The best configuration was using aluminum balls [25]. Moreover, other different designs of solar cookers are described and thermally analyzed in recent papers by Saxena and Agarwal [24] and Saxena et al. [25].

Solar cookers are aimed at reaching a safe cooking temperature and time depending on the food type. Furthermore, any solar cooker device should include the analysis of the following [26]:

- (i) The possibility of cooking at any time of day
- (ii) Cooking time must be comparable with conventional cooking
- (iii) Nutritional characteristics
- (iv) Sensory perception
- (v) Economic aspect

Solar weather conditions make cooking a difficult task. The standard prescribed temperature in solar cooking of most dishes is 70°C, which the food should attain and keep at that value for a minimum of 2 minutes [27]. The lower limit of cooking temperature is 62.8°C [28] to avoid degradation of cooked food due to the activity of remnant microorganisms. Nevertheless, in most cases, this temperature for cooking is reached after two hours of solar heating [29, 30], creating a favorable ambient for microorganisms growing. Therefore, the research works are focused on improving the thermal efficiency, the energetic efficiency, the efficacy, and CO<sub>2</sub> emission reduction [31–34]. However, the thermal effects and thermal history may affect cooked food's sensory and nutritional properties. Then, extreme care is necessary for process design to avoid subprocessing and overprocessing the meals in solar cookers. Thus, thermal process optimization is extremely desired [35]. Thus, thermal effect analysis on food properties is highly desired. Therefore, the quality analysis of the cooked product should be incorporated for better acceptance of the solar technology and to know how we can improve the solar cooking process [36–38]. A significant difficulty in performing the nutritional analysis of solar-cooked food is that the weather conditions: solar irradiance, wind velocity, air density, wind direction, ambient temperature, and their daily seasonal variations all strongly affect the functionality of the solar cooker and hence of the cooked dish as well [22]. This limitation can be surpassed by using a hybrid-solar cooker [39]. Also, it is possible to cook at any time of the day.

In previous work, we evaluated the sensory properties and consumer preferences of dishes cooked in hybrid solar cookers. We use an acceptance test with a five-point hedonic scale (excellent (5), good (4), regular (3), bad (2), and terrible (1)) and a rank-ordering method with untrained and trained panelists. In ten different dishes, the consumers did not find differences in the smell, color, texture, and appearance [40, 41]. We tested for over a decade many types of *tamal* dishes

prepared using the hybrid-solar cooker and found them palatable [42, 43]. However, a specific variety of *tamal*, the “elote tamal,” tasted bitter. *Elote tamal* is prepared from ground tender corn kernels, sugar, fresh milk, and butter. *Elote* means tender corncob; and *tamal* is from *tamalii*, which in the Aztec epoch meant “wrapped food.” The bitter taste in the “elote tamal” was eliminated by raising the initial temperature of cooking by activating the electrical heating element of the hybrid-solar cooker, which prevented fermentation of the milk-dough mix in the *tamal*. We report here an analysis of the nutrient contents in *elote tamales* prepared in the hybrid-solar cooker and traditional methods to understand the underlying processes causing differences in the solar-cooked dish. We developed the right strategy to prevent the bitter-taste-forming process with such understanding. We evaluate and compare *elote tamales* on the chemical composition: protein (total nitrogen), total fat, moisture content, ash, sodium, total reducing sugars, crude fiber, color, and acidity. The methodology developed here for cooking milk-based meals in a solar cooker applies to similar dishes. Our work suggests that milk-based dishes may present fermentation in solar cookers with a slow heating process. Nonetheless, a caveat of this work is that our hybrid solar cooker has not been characterized using a standardized methodology [31].

With the electricity grid and bright sun available in most regions of Mexico throughout the year, the hybrid solar-electric (H-S) cooker is widely accessible. This cooker eliminates the uncertainty of cooking a dish for the day’s main meal at 14:00 hrs (in Mexican tradition, after an early breakfast, the main meal is at 14:00–15:00 hrs, followed by a light meal at night. The results on H-S or traditionally cooked *elote tamales* were done at our Institute to correspond to the 14.00 h main meal).

This work is organized as follows: we describe the specifications of the H-S cooker and the preparation method for the *tamal*. Results on the qualitative and quantitative aspects of the nutritional properties of the *tamal* follow. We find that under the standard operation of the H-S cooker, the *elote tamale* is sour bitter *tamales*. We discuss the role of the moisture content, total reducing sugar, and titratable acidity based on physicochemical facts or hypotheses. In the section modified H-S procedure, we present a modification of the standard H-S solar cooking procedure to avoid the sour flavor and confirm that during the slow heating part of the cooking in the H-S cooker, the *tamales* undergo fermentation. Finally, we conclude by highlighting our findings.

### 3. Hybrid-Solar Cooker Description

We used the H-S cooker [39, 41] for cooking experiments; see Figures 1(a) and 1(b). This design is patented in Mexico. The solar cooker with electric backing used in this paper comprises a half-cylinder-shaped cooking chamber cut lengthwise on the longitudinal axis [39]. The chamber is thermally isolated by the wall and the cylinder caps and by a transparent material located lengthwise on the axial axis. A solar concentrator includes four flat mirrors angularly adjustable about the flat transparent glass. The glass is located at the upper portion of the solar concentrator. Thus, the device includes a stationary

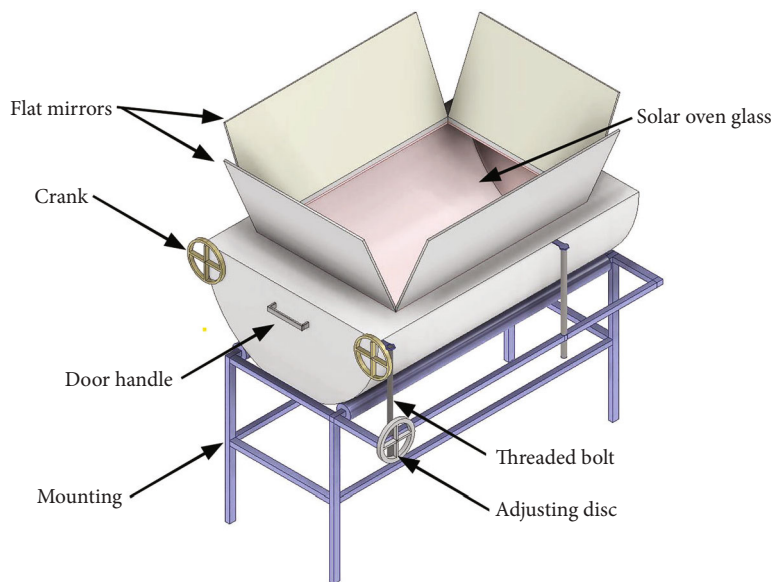
horizontal base, a semicircular support rotating over the base, a worm connected to the base and the semicircular support for fixing and switching the position of the support, and a bar connected to the end portions of the support, which allows the said bar to rotate over the axis to rotate the cylinder and to provide the accurate tracking of the sun during the annual movement [44]. The apparatus, oriented with the cylindrical axis perpendicular to the North-South axis of the earth, requires only a slight rotating movement over the bar to change the glass surface angle and concentrate the sunlight during a whole day, inside the cooking chamber, i.e., with only two degrees of freedom for tracking all year around. This mechanical system is provided for adjusting the tilt of the solar collector in such a manner that the flat transparent glass is a perpendicular surface to the direct solar radiation flow every day all year around (Table 1).

The energy concentration system is formed by four flat mirrors ( $0.74 \times 0.91$  m). The angle of the mirrors is  $55^\circ$  from the horizontal plane (glass cover) for the north and south mirrors,  $75^\circ$  for the west mirror, and  $35^\circ$  for the east mirror. The incident solar energy flux passes through the sheet glass (thickness 0.006 m) and is collected (about 80%) [43] inside the cooking chamber, involving the greenhouse effect due to the glass cover. Consequently, the solar heating process uses both mirrors and the greenhouse effect. The cooking chamber is a semicylindrical shape appropriate for a rotational system. The axis of the cylindrical chamber is placed perpendicular to the geographical north-south direction. Inside the chamber is a flat griddle with wheels under it to maintain the cooking pots (food containers) in the correct position. This system allows the pots to move according to the cooking chamber’s curvature, preventing food spillover from its container.

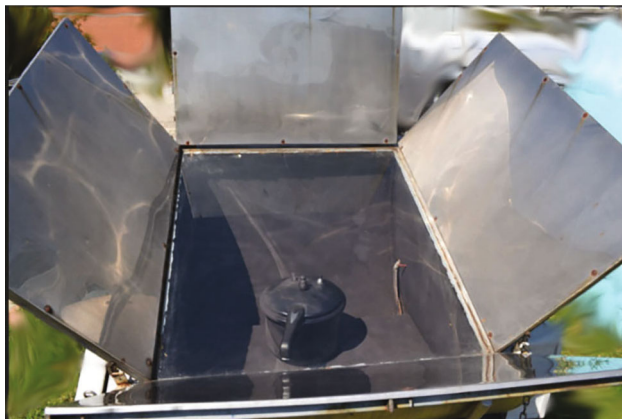
The mechanical system for altering the angle of the chamber includes a threaded bolt and an adjusting disc. We can rotate the adjusting disc manually every week to obtain the desired angle from  $-10$  to  $60^\circ$ . We set the angle according to the latitude of the geographical zone of Temixco, Morelos (latitude of  $18^\circ 50' N$  and longitude of  $99^\circ 14' W$ ), where all the experiments were carried out. A weekly adjustment was made to obtain nearly perpendicular solar incidence on the glass cover. Suppose the solar energy is insufficient to reach the desired temperature. In that case, a control device starts backup electric resistance heaters of 1 KW each to meet the desired set temperature [13, 39].

The cooking chamber’s capacity is three pots of 6 L. In this work, we use only one pot. The pots are introduced into the chamber through a lateral door. The design includes a rubber door seal to prevent heat loss. The door can be closed manually with two lateral cranks. The chamber is insulated with glass fiber padding (thickness of 0.065 m).

The hybrid-solar cooker works with solar radiation or switch-on the electric resistances heating the chamber to reach the selected cooking temperature. With the temperature selection, we wanted to analyze if the higher cooking temperature affects the sour flavor. Still, as we see later, the temperature does not affect the nutritional properties. Thus, in the final experiment, we used only the lowest temperature. Once the desired cooking temperature is reached, the cooker may work with solar irradiance alone.



(a)



(b)

FIGURE 1: Hybrid-solar cooker: (a) schematic and (b) used device, details in Tapia-Salinas et al. [39].

TABLE 1: Specifications of the solar cooker.

Component	Width	Length	Characteristic
North mirror	0.74	0.91	55°*
South mirror	0.74	0.91	55°*
Est mirror	0.84	0.91	35°*
West mirror	0.84	0.91	75°*
Glass	0.83	0.73	0°*
Cooking chamber	1.01	1.00	18 L**

\*From the horizontal plane. \*\*Capacity.

The temperature control system consists of thermocouples that sense the chamber temperature. An Arduino Yun plate that runs our code instructions and sets the temperature by switching on/off the electrical resistances when needed. Using the communication capabilities of this device (WiFi), we send the data to a microcomputer, where we analyze and process the temperature data of the chamber. The temperature

monitoring/control/recording was made at one-minute intervals. We use data from the solarimetric station of the Instituto de Energías Renovables to report the weather conditions: ambient temperature, direct solar irradiance, diffuse solar irradiance, global solar irradiance, relative humidity, and wind speed. All data were collected every 10 min and processed by the meteorological station ESOLMET-IER-UNAM ([http://esolmet.ier.unam.mx/Tipos\\_consulta.php](http://esolmet.ier.unam.mx/Tipos_consulta.php)). Figure 2 shows the temperature profile inside the cooking chamber in the H-S cooker for the three selected cooking temperatures. Electrical power is used mainly in the fast heating process. After reaching the selected temperature in the chamber, the H-S cooker runs almost solar.

#### 4. Methods

We describe here the materials and procedure to prepare *tamal*, according to Mexican tradition, and the differences between traditional and H-Solar procedures. Also, we describe the methods used to determine protein (total



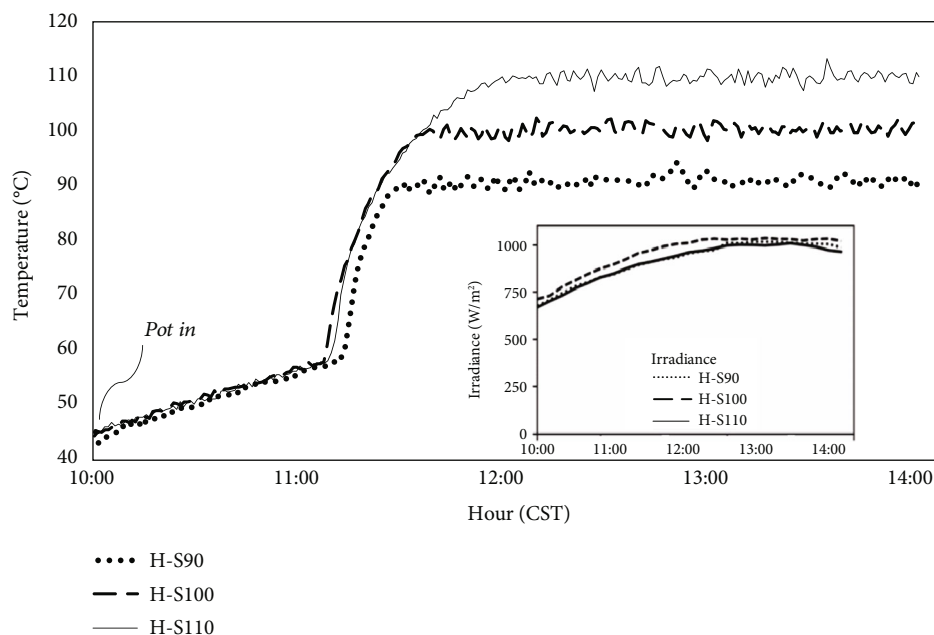


FIGURE 2: Typical temperature curves we observed in the hybrid-solar cooker 90°C, 100°C, and 110°C. In the inset, we are plotting the solar irradiance (source: own elaboration).

nitrogen), crude fat, moisture content, ash, sodium, total sugars, crude fiber, titratable acidity, and color of the *tamales*.

**4.1. Elote Tamal Preparation.** We bought corn dough prepared from fresh-plucked corncobs (called *elote*), butter, salt, sugar, baking powder, and cow milk from the local market in Temixco, Morelos, Mexico. We followed the traditional recipe (*Istmous of Tehuantepec elote tamales*) as follows: raw corn dough (500 g), butter (100 g), cow milk (75 mL), sugar (40 g), baking powder (7.5 g), and salt (1 g). The raw corn, cow milk, and butter were mixed for 3 min using a blender (Oster, 6662). Gradually, we added sugar, baking powder, and salt to obtain a creamy paste. This creamy paste is called corn dough. We divided the past into portions of 144 g each, in cylindrical forms (resembling baguettes), and placed them on dried raw cornhusk and wrapped them. These cornhusks are available locally, collected during the corn harvest, and preserved for preparing *tamal* throughout the year. We prepared sets of five *tamales* to perform all the different trials. The cooked tamales were stored in a freezer at 4°C for three days before the nutritional analysis. This step kept the food sample out of the danger zone (between 8°C and 60°C [27]) and prevented bacterial growth. We performed different trials on different days. These trials consisted of varying the cooking temperatures, as explained below.

**4.2. Traditional Cooking.** For *tamales* traditional cooking, we used a commercial pot (Taurus, EDIPO, China) with a 15.5 cm height, 0.3 cm thickness, and 22.5 cm diameter. The *tamales* were placed over a metal grid inside the pot. We used 1 L of water, with the water level 5 cm below the grid, for vapor-cooking the *tamales*. The lid was used without sealing. The cooking lasted for 40 min. In H-S cooking,

we adapted to cooking time as described below. Because Temixco, Morelos, Mexico, is 1300 meters above sea level, the cooking temperature was 95°C. The cooking lasted for 60 min.

**4.3. Hybrid-Solar Cooking.** In the hybrid-solar cooker (Figure 1), we can adjust the time when it uses only solar radiation to heat the meals. In addition, we can select the maximum temperature for cooking. We fix the solar heating time as 1 hour (10:00–11:00 h local).

We place a black “express pot inside the hybrid-solar cooker” (Taurus, EDIPO, China). The pot was previously painted black for better solar irradiance absorption. One liter of water was added for vapor cooking in the same manner as in the traditional cooking method. The pot was sealed for solar cooking, and the five *tamales* were placed in the same manner as in the traditional procedure.

Based on our experience with other meals, we fixed the solar cooking period to 1 hour. To assure well-cooked *tamales*, in all cases, the *tamales* were inside the pot for 3 hours. In Figure 2, we show the representative temperature evolution for the three solar cooking cases: H-S90 at 90°C, H-S100 at 100°C, and H-S110 at 110°C. In these curves, we can see that after reaching a temperature of nearly 55°C after 1 h under the sun (11:00 h local), the electrical backup starts, which sets in an abrupt increase in the slope of the curve, until the set temperature in the control device was reached. At 14:00 h local time, experiments were finished (Figure 3).

The following section describes the standard methods and analysis techniques for nutritional properties, color, and titratable acidity determination. These were selected following the international standards on the Official Methods of Analysis [45].

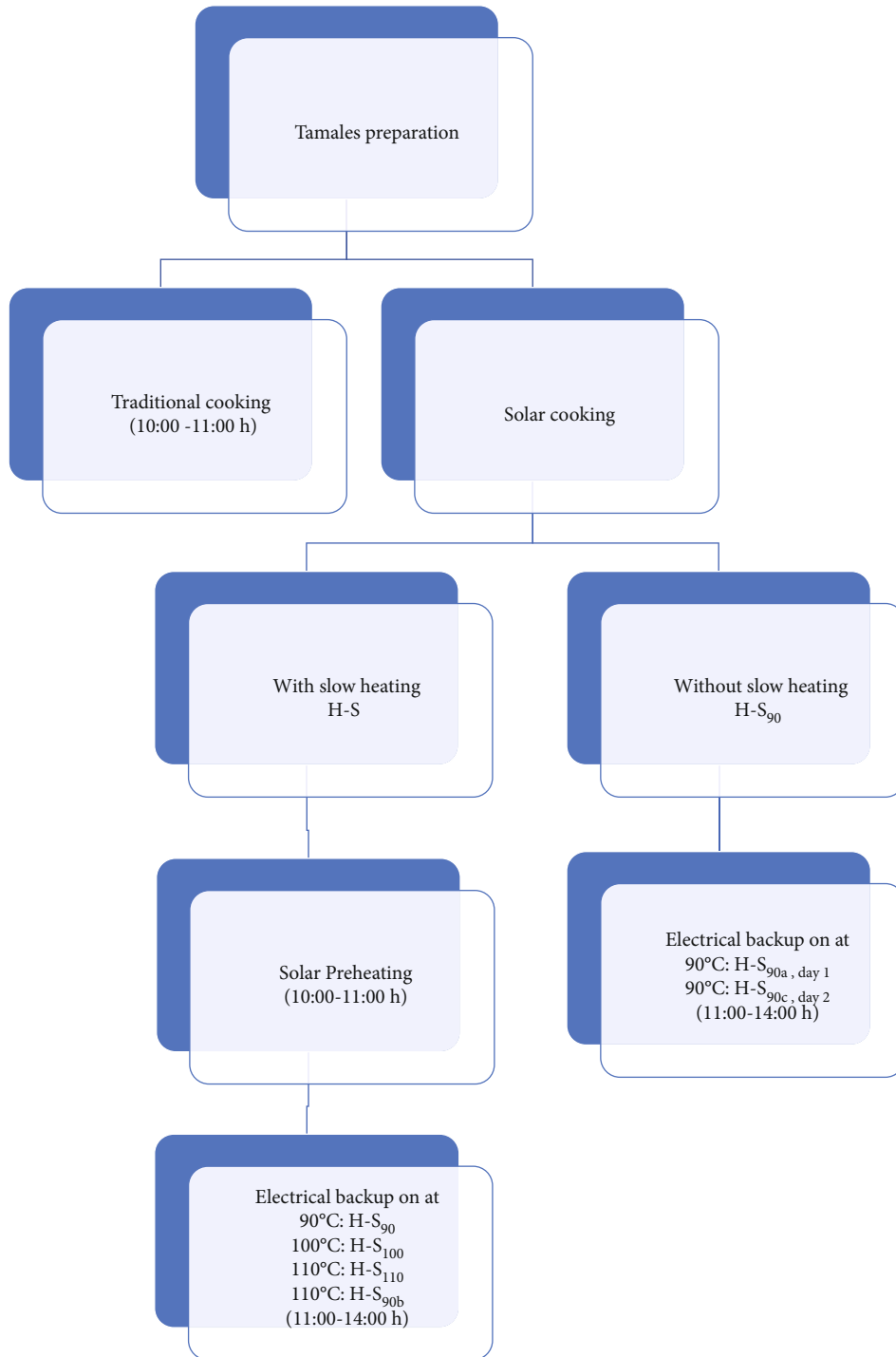


FIGURE 3: Diagram for hybrid-solar cooking process with slow heating (H-S) and without slow heating (H-S90).

**4.4. Nutritional Properties.** We present the methodologies used in this work to evaluate the nutritional properties of *tamales*, based on official methods. The evaluated properties are the moisture content (930.15), crude fat (2003.05), protein as total nitrogen (2001.11), ashes (942.05), crude fiber (962.09), sodium trough chloride (Mohr's method), and total reducing sugars (Lane-Eynon's method); carbohydrates were obtained by a difference of 100.

**4.5. Color Determination.** We measure the color according to CIELAB indices (International Commission on Illumination, Vienna) using a colorimeter (Kingwell, JZ-300, China). We determine Luminosity  $L^*$  and two parameters that indicate chromaticity, namely,  $a^*$  and  $b^*$ . The first chromaticity parameter indicates redness ( $+a^*$ ) to greenness ( $-a^*$ ), and the last one refers to yellowness ( $+b^*$ ) to blueness ( $-b^*$ ). The *tamal* samples were ground with a

TABLE 2: Proximal analysis of corn *tamales*. T-95: traditional cooking at 95°C; H-S90, HS100, and HS110: solar cooking at 90, 100, and 110°C, respectively; H-S90<sub>a</sub>: at 90°C without slow heating, day 1. H-S90<sub>b</sub>: at 90°C slow heating, day 1. H-S90<sub>c</sub>: at 90°C without slow heating, day 2.

Procedure	Moisture	Ashes	Chlorides	Reducing sugar	Protein	Crude fiber	Crude fat	$L^*$	$a^*$	$b^*$
T-95	67 ± 1	1.25 ± 0.04	0.12 ± 0.02	6.3 ± 0.7	3.5 ± 0.1	1.1 ± 0.2	7.7 ± 0.6	68 ± 1	-0.7 ± 1	14 ± 2
H-S90	63 ± 2	1.29 ± 0.04	0.13 ± 0.01	4.9 ± 0.1	3.4 ± 0.2	1.1 ± 0.1	7.6 ± 0.9	67 ± 2	2.5 ± 0.5	19.2 ± 0.1
H-S100	62 ± 2	1.17 ± 0.07	0.10 ± 0.01	5.0 ± 0.4	3.5 ± 0.2	1.1 ± 0.1	7.9 ± 0.7	66 ± 4	1.9 ± 0.2	18 ± 1
H-S110	65 ± 1	1.20 ± 0.08	0.10 ± 0.01	4.7 ± 0.2	3.3 ± 0.2	1.1 ± 0.1	7.9 ± 0.3	67 ± 1	3.0 ± 0.1	20.4 ± 0.4
H-S90 <sub>a</sub>	62 ± 1	1.24 ± 0.06	0.10 ± 0.01	5.2 ± 0.1	2.9 ± 0.1	0.6 ± 0.1	12.5 ± 0.4			
H-S90 <sub>b</sub>	62 ± 2	1.25 ± 0.07	0.09 ± 0.004	4.7 ± 0.1	2.8 ± 0.1	0.6 ± 0.1	12.7 ± 0.2			
H-S90 <sub>c</sub>	60 ± 2	1.16 ± 0.08	0.09 ± 0.01	5.0 ± 0.1	2.4 ± 0.1	0.4 ± 0.1	12.2 ± 0.5			

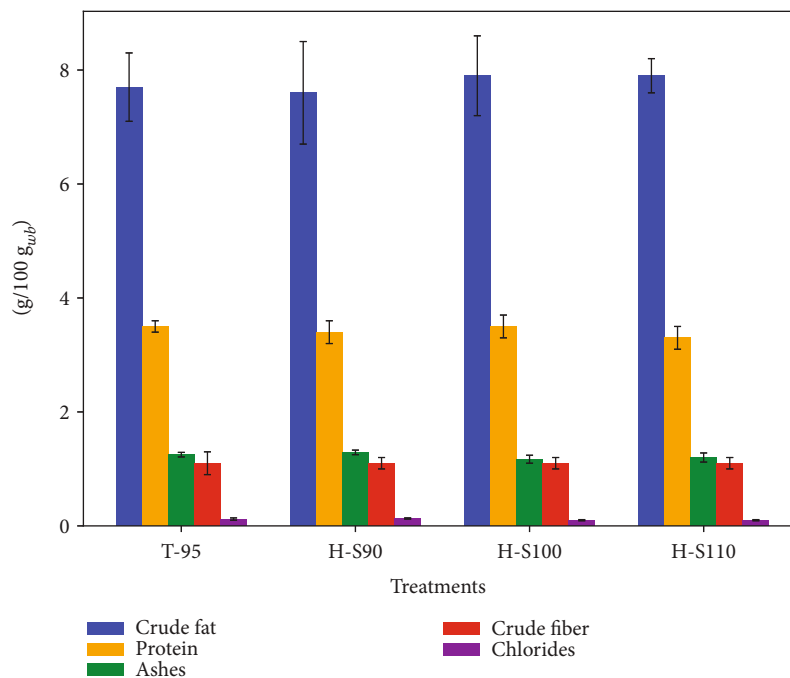


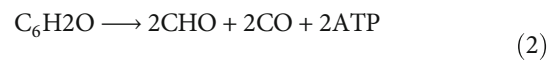
FIGURE 4: Nutritional analysis (ash, chloride, protein, crude fat, and crude fiber) of samples of corn *tamales* subjected to hybrid-solar cooking processes (H-S90, H-S100, and H-S110°C), and conventional (T-95°C). Right axis (protein and crude fat). Left axis (ashes, chlorides, and crude fiber).

mortar to homogenize them for analysis. The samples were placed into a Petri container (diameter: 3 cm) under the colorimeter view with an LED source. The scattered light from the sample provided for directional annular 45°, illumination source/0°, measurements using the colorimeter. With this simple procedure, we can determine the total color difference ( $\Delta E$ ) by using the following relationship (de [46, 47]):

$$\Delta E = \sqrt{\Delta L^{*2} + \Delta a^{*2} + \Delta b^{*2}}, \quad (1)$$

where  $\Delta$  indicates the differences among  $L^*$ ,  $a^*$ , and  $b^*$ . If  $\Delta E > 3$ , the colors present a strong difference; if  $1.5 < \Delta E < 3$ , the colors between two samples are different; if  $\Delta E < 1.5$ , the colors are considered similar [47].

4.6. *Titrateable Acidity.* The lactic acid fermentation consists of converting sugars into lactic acid as the following reaction [48]:



Glucose  $\longrightarrow$  lactic acid + carbon dioxide + energy.

In our experiments, we expect an acidity increase due to fermentation led by a low-heating process. Therefore, we measure the titrateable acidity of the tamales. We determine the titrateable acidity according to the Official Method of Analysis (947.05) [45].

4.7. *Heat Transfer Analysis.* We calculate the accumulated energy  $E_{ac,T}$  inside the solar cooker.

$$E_{ac,T} = E_{in,T} - E_{out,T}, \quad (3)$$

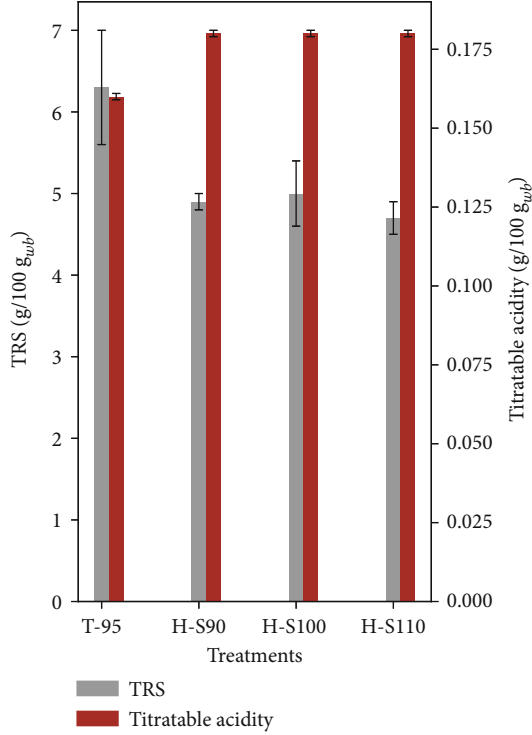


FIGURE 5: TRS and titratable acidity of samples of corn *tamales* subjected to hybrid-solar cooking processes (H-S90, H-S100, and H-S110°C) and conventional (T-95°C). Right axis (TRS). Left axis (acidity).

TABLE 3: Color measurements ( $L^*$ ,  $a^*$ , and  $b^*$ ) in *elote tamales*. T-95: traditional cooking at 95°C; H-S: solar cooking at 90, 100, and 110°C.

Procedure	$L^*$	$a^*$	$b^*$
T-95	68 ± 1	-0.7 ± 1	14 ± 2
H-S90	67 ± 2	2.5 ± 0.5	19.2 ± 0.1
H-S100	66 ± 4	1.9 ± 0.2	18 ± 1
H-S110	67 ± 1	3.0 ± 0.1	20.4 ± 0.4

where the  $E_{in,T}$  is the input energy supplied by the sun and  $E_{out,T}$  is the energy loss. For the input energy, we use

$$E_{in,T} = A_{sup,c} \eta_{dir,c} \eta_{tr} \left[ \underbrace{E_{ext}(n) e^{(-B/\cos \theta_z)} \cos \theta}_{\text{Direct-flux-energy}} + \underbrace{AC e^{(-B/\cos \theta_z)}}_{\text{Diffuse-flux-energy}} \right], \quad (4)$$

where the  $A_{sup,c} = 1.08 \text{ m}^2$  is the area including the four mirrors;  $\eta_{dir,c} = 0.82$  is the concentrator efficiency;  $\eta_{tr} = 0.92$ , is the transmission efficiency of the glass;  $A$  and  $B$  are constants for the experimental data adjustment. For March, the values of the constants are  $A = 1186 \text{ W/m}^2$ ,  $B = 0.156$ , [43].  $\theta_z = 22.5^\circ$  is the solar angle;  $E_{ext}(n)$  is the relationship

TABLE 4: Weather conditions. T-95: traditional cooking at 95°C; H-S90, HS100, and HS110: solar cooking at 90, 100, and 110°C, respectively; H-S90<sub>a</sub>: at 90°C without slow heating, day 1. H-S90<sub>b</sub>: at 90°C slow heating, day 1. H-S90<sub>c</sub>: at 90°C without slow heating, day 2.

Procedure	Ambient temperature (°C)	Wind speed (m/s)	Irradiance (W/m <sup>2</sup> )
H-S90	28 ± 2	2 ± 0.7	890 ± 47
H-S100	27 ± 2	2.3 ± 0.8	929 ± 43
H-S110	28 ± 2	2.3 ± 0.8	868 ± 35
H-S90 <sub>a</sub>	27 ± 1	1.8 ± 0.6	702 ± 173
H-S90 <sub>b,c</sub>	27 ± 1	1.4 ± 0.4	767 ± 49

of external energy dependent on the day's number.

$$E_{ext}(n) = \frac{\hat{S} [1 + \varepsilon (\cos [(n-2)(360^\circ/365.2)])]^2}{1 - \varepsilon^2}, \quad (5)$$

where the  $\hat{S} = 1343 \text{ W/m}^2$  is the solar constant,  $\varepsilon = 0.01672$  is the orbital eccentricity, and  $n$  is the number of the day into the year. The lost energy by conduction/convection and radiation  $E_{out,T}$  was calculated using the following equation:

$$E_{out,T} = \frac{T - T_{amb}}{R_{Total}}, \quad (6)$$

where  $T$  is the temperature of the walls,  $T_{amb}$  is the ambient temperature, and the total is the total resistance that includes walls and the glass and mirrors  $R = 0.13 \text{ K/W}$  [43].

**4.8. Statistical Analysis.** We perform all the experiments in triplicate to achieve reproducible experiments and results. We set a randomized test sequence to prevent the experiment's effects on unknown variables like the weather (wind speed, ambient temperature, and solar irradiance) and uncontrolled variables (grain size, growing conditions). Thus, to analyze the influence of the cooking pathway (one factor), with four levels (treatments  $T$ : traditional cooking (T-95) at 95°C, H-S90: hybrid-solar cooking at 90°C, H-S100: hybrid-solar cooking at 100°C, and H-S110: hybrid-solar cooking at 100°C), in the nutritional properties, we perform a single-factor analysis of the variance (ANOVA) [49]. Statistical significance is the probability of observed differences between the experimental units. The variations may be identified when the calculated probability exceeds the chosen significance levels. Suppose the calculated probability is greater than the chosen significance levels. In that case, the treatments have no significant differences, or all treatments' effects are statically equivalent. In this study, we use a significance level  $\alpha = 0.05$ . We use NCSS 2019 trial software for the comparison of the variances. The results and discussion are described in the next section.

## 5. Results and Discussion

We present the results of the five different experimental sets to analyze the nutritional properties of *tamales*. The following subsection contains the results on conventional cooking versus H-S cooking. We observe that the ash,



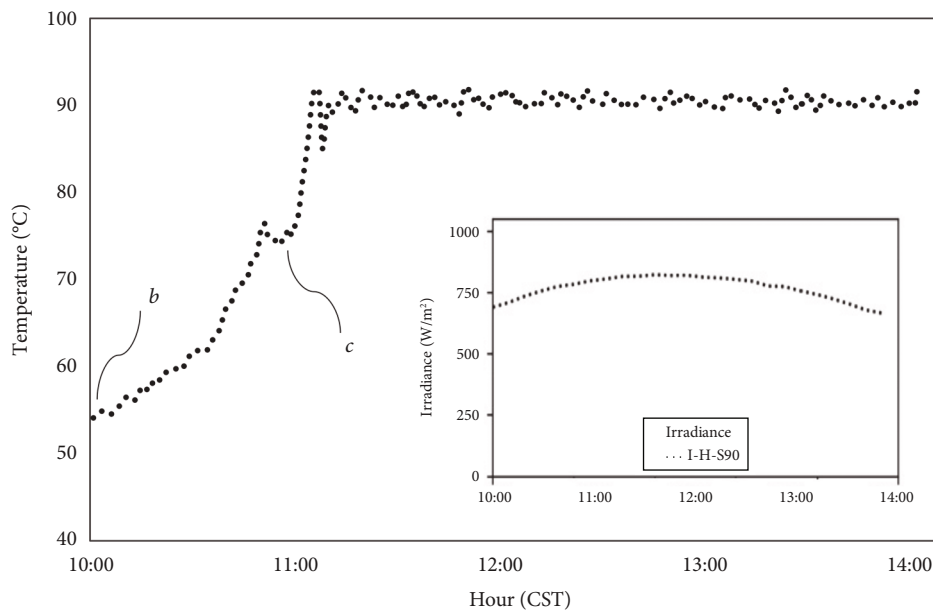


FIGURE 6: Typical temperature curves in the H-S cooker. The time at which the raw tamales in the pot are introduced in the chamber in b and c is indicated in H-S90<sub>b</sub> and H-S90<sub>c</sub> plots. In the inset, we are plotting the solar irradiance.

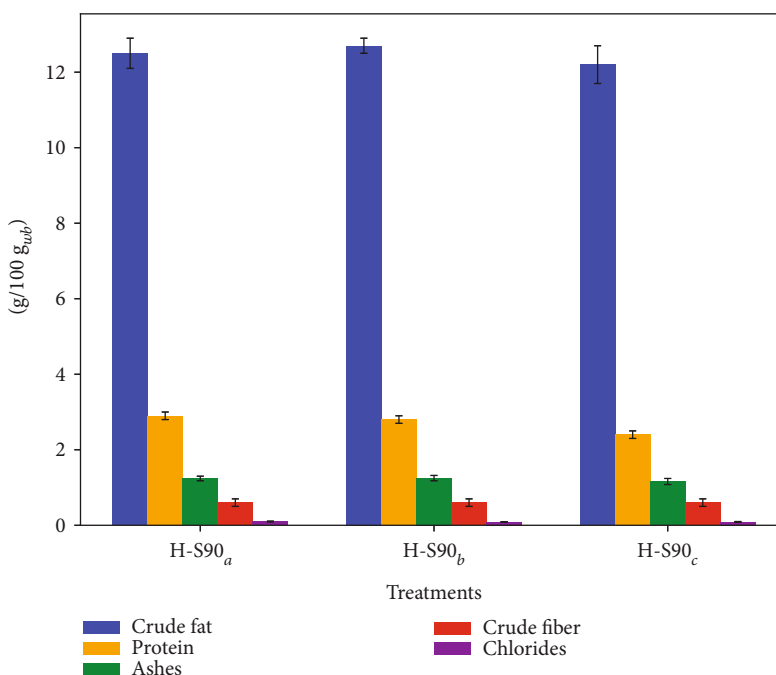


FIGURE 7: Nutritional analysis (ash, chloride, protein, crude fat, and crude fiber) of samples of corn *tamales* subjected to hybrid-solar cooking: processes without a slow heating period (H-S90<sub>a</sub> and H-S90<sub>b</sub>) and with a slow heating period (H-S90<sub>c</sub>). Right axis (protein and crude fat). Left axis (ashes, chlorides, and crude fiber).

chloride, protein, crude fat, and crude fiber results have no differences. In contrast, the samples' moisture, sugar, and titratable acidity present significant changes that deserve discussion. We show all the data in Table 2.

5.1. Proximal Analysis. In Figure 4, we summarize the results of the proximal analysis of *tamales* cooked in the traditional method (T-95: at 95°C) and in the H-S procedures (H-S90:

hybrid-solar cooking at 90°C, H-S100: hybrid-solar cooking at 100°C, and H-S110: hybrid-solar cooking at 110°C). We do not find significant differences ( $\alpha = 0.05$ ) in the nutrient analysis (ash, chloride, protein, crude fat, and crude fiber) among the four treatments (T-95, H-S90, H-S100, and H-S110). From a nutritional point of view, equivalent contents of proteins grants imply that the essential amino acids contained in maize [50] are available to be consumed. Thus,

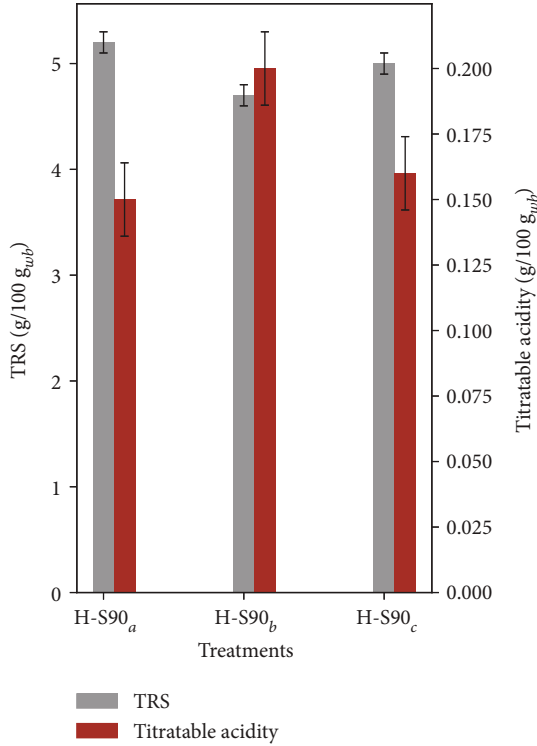


FIGURE 8: TRS and titratable acidity of samples of corn *elote tamales* subjected to hybrid-solar cooking: processes without a slow heating period (H-S90<sub>a</sub> and H-S90<sub>c</sub>) and with a slow heating period (H-S90<sub>b</sub>). Right axis (TRS). Left axis (acidity).

TABLE 5: The solar cooker's accumulated energy, ganged energy, and energy loss.

Experiment	$T_{amb}$ (°C)	$T$ (°C)	$E_{in,T}$ (W)	$E_{out,T}$ (W)	$E_{ac}$ (W)
H-S90	25	58	924	254	670
H-S100	24	56	923	246	677
H-S110	25	59	923	261	662

all samples are nutritionally adequate. However, we find significant differences in moisture content, reducing sugars, titratable acidity, and color, as shown in Figure 5 and Table 2. We will discuss them in detail in the next subsections.

**5.2. Moisture Content.** We present the moisture contents of the *tamales* from all experiments in Table 2. The average moisture content of tamales from traditional cooking is higher than that from hybrid-solar cooking. According to Duncan's multiple comparison test, with  $\alpha = 0.05$ , the moisture content in the *tamal* from traditional cooking is distinct from those in samples processed with H-S90, H-S100, and H-S110 procedures. We observe that the moisture contents obtained in this work are the same as previous results (54–64 g/100 g) [2].

**5.3. Color.** We present the color parameters of the *tamales* in Table 3. The value of  $b^*$  for the *tamal* from traditional cooking is statistically different from those made in the H-S pro-

cedures. The standard deviations are minor. These significant differences in  $b^*$  can be due to the nonenzymatic browning in the samples cooked in the H-S cooker. In addition, we find a shift to red ( $a^*$ ) of *tamales* from H-S procedures compared with that of traditional *tamal*. The parameters  $a^*$  and  $b^*$  indicate a browning shift in *tamales* cooked under the H-S procedure. The Maillard reactions occur when the reducing sugars, like glucose, unite to a free amino group (amino acid or protein), and human eyes can detect these reactions through red-shift and yellow-shift of the color, as noted here.

This qualitative behavior is rendered quantitative when we calculate the  $\Delta E$  values for the *elote tamales* from the three H-S procedures compared with that from the traditional cooking:  $\Delta E_{T-95:H-S90} = 6.2$ ,  $\Delta E_{T-95:H-S100} = 5.5$ , and  $\Delta E_{T-95:H-S110} = 7.4$ . All these values indicate that H-S procedures have different colors than traditional ones. The corresponding color differences within the H-S procedures are  $\Delta E_{H-S90:H-S100} = 1.8$ ,  $\Delta E_{TH-S100:H-S110} = 2.9$ ,  $\Delta E_{H-S900:H-S110} = 1.3$ , which indicate that the color differences are not so evident, but the human eye can detect it.

**5.4. Total Reducing Sugars.** We find that the total reducing sugars (TRS) contents in *elote tamales* from the H-S procedures are smaller than the corresponding for the traditional procedure (Figure 5). This sugar content is within the interval labeled in commercial corn *tamales* produced by the traditional route: “La Costeña,” 8.18 g/100 g, and “La Michoacana Meat Market”, 5 g/100 g [51, 52]. We note that during the slow heating time in the H-S procedure, the temperature is below 57.6°C. Because raw corn could contain some microorganisms, they can reduce the sugar in the milk and acidify the *tamal*. For example, these may include *Streptococcus thermophilus*, which produces the lactic acid, *Lactobacillus thermophilus*, and results in the acidity in the dough-mix in the temperature range of 37–50°C [53]. Also present in the mix is *Lactobacillus plantarum* [54], a natural microorganism of corn used in the natural fermentation of different alcoholic drinks.

In Figure 2, we show that during the first hour of cooking, the temperature increases from 20 to 57°C under high moisture content. This temperature increase enhances the growth of microorganisms, leading to a reduction in the TRS. We also observe a reduction in acidity. We find an unpalatable bitter flavor in *tamales* from the H-S procedure, which is not the case with the *elote tamales* from the traditional method. We carefully examine the titratable acidity measurements to understand the difference among these *elote tamales*.

**5.5. Titratable Acidity.** We show the titratable acidity of the *tamales* in Figure 5. As reference data, the titratable acidity in cow milk reported in the literature is 16.8°TH [55] 0~0.15%. Significant differences exist in the parameter among *tamales* from the traditional cooking and H-S procedure. The high value in titratable acidity and the lower sugar content in *tamales* obtained in the H-S procedure suggest that their bitter flavor arises from the fermentation that occurs during a slow rate of increase in temperature in the

TABLE 6: The solar cooker's accumulated energy, ganged energy, and energy loss.

Experiment	$T_{amb}$ (MJ/ $Kg_{fp}$ )	GAS req ( $Kg_{lp}/Kg_{fp}$ )	Cost of the fuel (dollars)	Energy cost saved (dollars)	CO <sub>2</sub> non emitted ( $kg_{CO_2}/kg_{fp}$ )
T-95	6.11	0.34	1.08	0.37	1.00
H-S90	3.37	0.10	1.08	0.11	0.29
H-S100	3.38	0.10	1.08	0.11	0.29
H-S110	3.36	0.10	1.08	0.11	0.29

\*Cost of LP gas (\$/Kg<sub>Gas</sub>) (<https://www.cre.gov.mx/ConsultaPrecios/GasLP/PlantaDistribucion.html?idiom=es>).

solar cooking process. This last conjecture is based on the Mexican standard for raw milk (NOM-155-SCFI-2012), where fermented milk has titratable acidity higher than 0.17%. Thus, to prevent fermentation, avoid the bitter flavor, and thereby improve the quality of H-S *tamales*, we can introduce the *tamales* placed in the pot into the S-H cooking chamber only after the solar heating process has elevated the temperature adequately. Thus, the cooking temperature promptly rises above 60°C which is not conducive to fermentation. We will discuss our findings in the next section.

## 6. Modified H-S Procedure

We designed a set of experiments to test our conjecture that the fermentation occurred in the H-S *tamales* during the slow solar heating stage. (a) First, we start heating the H-S cooker without any pot, i.e., the chamber receives the sun rays and is heated while empty, without meals or a pot inside. We let this empty heating period run for an hour, from 10:00 am to 11:00 am, which elevates the chamber's temperature to approximately 60°. Then, we introduce the pot with the stacked raw *elote tamales* inside the H-S cooker and put on the electric backup to rapidly reach the cooking temperature, compensating for the chamber's cooling down while opening and closing. (b) In the second experiment, we start the heating procedure at 10:00 am with the raw "elote tamales" in the pot already placed inside the chamber. Thus, the raw tamales would experience a slow heating procedure until 11:00 when the electric backup heater goes on, and the temperature increases to roughly 90°.

We run additional experiments on the same day to ensure identical weather conditions. In the previous section, we have presented and discussed the results for H-S90, which is the same as (b) but on a different day, and the weather conditions are in Table 4. This section presents the results for experiments (a) and runs under the same weather conditions (b). We refer to this experiment (a) under simultaneous day conditions as (c) to denote such a difference. The difference between (b) and (c) is that (c) does not experience slow heating, but in both cases, they received the same fast heating processes under the same weather conditions. The difference between (a) and (c) is that they are done on different days and in weather conditions. It is a piece of relevant information that Temixco borders with Cuernavaca City, which is called "the city of the eternal spring" (Ciudad de la Eterna primavera <https://en.wikipedia.org/wiki/Cuernavaca>); the temperature and solar

irradiance variation during the day did not vary markedly on the days we performed these experiments Table 4.

The temperature profile in the chamber for these experiments, in Figure 6, shows that the fast heating for H-S90<sub>b</sub> and H-S90<sub>c</sub> experiments compare well with that for case (a). With these procedures, we have three sets of *elote tamales* samples to compare. We perform the same statistical analysis on these samples, as discussed above. In all cases, the raw *elote tamales* were stored in a freezer at 4°C before placing them in the chamber for cooking in H-S90<sub>a</sub> and H-S90<sub>c</sub> *tamales* procedure.

In all experiments, we reach the lower limit of cooking temperature of 62.8°C [28], to avoid degradation of cooked food due to the activity of remnant microorganisms. This temperature is considered a safe temperature for cooking. Also, using express pots, as in classic cooking, ensures that the cooked meals are chemically and biologically safe as any other meals prepared in such bowls. In Figure 7, we do not notice significant differences in ash, chlorine, protein, total fat, and crude fiber contents in the H-S a, b, and c processes. However, we find significant differences in TRS and titratable acidity, as shown in Figure 8.

**6.1. Total Reducing Sugars (TRS).** We show the TRS's results in the *tamales* cooked at 90°C in the hybrid-solar cooker (H-S90<sub>a</sub>, H-S90<sub>b</sub>, and H-S90<sub>c</sub>) in Figure 8. The TRS for sample H-S90<sub>b</sub> was  $4.68 \pm 0.13$  (g/100 g), while, for the H-S90<sub>a</sub> and H-S90<sub>c</sub>, where there is no slow heating period, is  $4.98 \pm 0.07$  (g/100 g) and  $5.18 \pm 0.09$  (g/100 g), respectively. Although they have lower TRS contents in all these cases compared to the traditional procedure, they present no statistically significant differences among them (H-S90<sub>i</sub>). Let us move to titratable acidity features.

**6.2. Titratable Acidity.** We present the results in titratable acidity in Figure 8 for H-S cooking, H-S90<sub>a</sub>, and H-S90<sub>c</sub>, which are 0.15 and 0.16 (g/100 g), while for H-S90<sub>b</sub>, it is 0.20 (g/100 g). Thus, the acidity values for H-S90<sub>b</sub> and H-S90<sub>c</sub> are no different from that in tamales from traditional cooking. These values confirm that the milk acidification, which consequently acidifies the *elote tamal*, is due to an initial slow heating of raw tamales, leaving it at a low temperature conducive to fermentation. The bitter taste is avoided in milk-containing food prepared in solar cookers by not subjecting these to a slow solar heating period in conventional solar or solar-hybrid cookers. We showed that the bitter taste in *elote tamales* originates from the initial fermentation in the raw food at temperatures less than 60°C. The present

result confirms that slow solar heating in food with milk is not recommendable due to the possibility of fermentation.

6.3. *Heat Transfer.* The accumulated energy, ganged energy, and energy loss are shown in Table 5.

As we can observe, the energy gained from the sun reduces the electricity used for cooking. This hybrid solar cooking led to cooking inclusive on cloudy days. In our experiments, we can avoid the CO<sub>2</sub> emission for the partial substitution of electricity (Table 6).

## 7. Conclusions

This paper presents the preparation methods and nutrient analysis of *tamales* cooked in the hybrid-solar cooker compared with *tamal* from traditional cooking. From a nutritional point of view, we can conclude that *elote tamales* prepared in the hybrid-solar cookers are an alternative for home food processing. They are nutritionally adequate, as in tamales prepared by the traditional method. We found no significant differences in chlorine, ashes, total fat, protein, and crude fiber contents among these products. However, we have found significant differences in color, moisture content, TRS, and titratable acidity. After analyzing the aspects showing the differences, we found that in “elote tamal,” a slow heating process inherent in many solar cookers produces fermentation and diminishes the quality of the solar-prepared milk-based meal. In this work, we established that a simple modification in the cooking procedure eliminates such fermentation. This modification avoids the slow warming-up period by introducing the cooking pot with the raw food into the solar-heated chamber after it has reached 65°C. The result is good quality food without the sour taste offered in the traditionally cooked product. We emphasize that the results are relevant to the solar cooking of other milk-containing dishes. Raw food is liable for fermentation during the slow-heating period conducive to fermentation and should go into a solar cooker, which has already reached a temperature higher than 65°C, which inhibits this fermentation (avoids the bitter taste). This approach produces solar-cooked palatable and nutritious dishes as in traditional cooking. Solar cookers with an electric backup for a short time to compensate for cooling down during the opening and loading of the chamber or coming on during unexpected weather changes is a convenient option for the traditional method to encourage trying out many actual traditional recipes in solar cooking and to determine the adequate H-S cooking conditions.

## Data Availability

The data used to support the findings of this study are available from the corresponding author upon request.

## Conflicts of Interest

There is no conflict of interest.

## Authors' Contributions

Anabel López-Ortiz and Jesús A. del Río defined the problem and conceived the experiments. Arnold A. Hernández-Medina and Anabel López-Ortiz performed the experiments. Anabel López-Ortiz, Arnold A. Hernández-Medina, and Jesús A. del Río analyzed the results. All authors wrote and reviewed the manuscript.

## Acknowledgments

We thank Prof. P.K. Nair for enlightening comments on this paper. Also, Anabel López thanked Prof. Rosalinda Toledo Chiñas for the local recipe to make tamales and Nicolás Iván Román Roldán for the scheme of the solar cooker. This work was supported by the DGAPA-UNAM through project PAPIIT TA200320. Arnold A. Hernández Medina thanks CONACYT (Sistema Nacional de Investigadores) for the scholarship (EXP AYTE 18530 (I1200/16/2019)) through Dr. Jesús Antonio del Río Portilla.

## References

- [1] United Nations Educational, Scientific and Cultural Organization, “Representative list of the intangible cultural heritage of humanity: traditional Mexican cuisine,” 2010, <https://ich.unesco.org/en/RL/traditionalmexican-cuisineancestral-ongoing-community-culture-themichoacan-paradigm-00400>.
- [2] C. W. Weber, E. A. Kohlhepp, A. Idouraine, and L. J. Ochoa, “Nutritional composition of tamales and corn and wheat tortillas,” *Journal of Food Composition and Analysis*, vol. 6, no. 4, pp. 324–335, 1993.
- [3] R. M. Mariscal-Moreno, J. de Dios Figueroa Cárdenas, D. Santiago-Ramos, P. Rayas-Duarte, J. J. Veles-Medina, and H. E. Martínez-Flores, “Nixtamalization process affects resistant starch formation and glycemic index of tamales,” vol. 82, no. 5, pp. 1110–1115, 2017.
- [4] A. Q. Guzmán, M. E. Jaramillo Flores, J. S. Fera, and M. G. Méndez Montealvo, “Effects of polymerization changes in maize proteins during nixtamalization on the thermal and viscoelastic properties of masa in model systems,” *Journal of Cereal Science*, vol. 52, no. 2, pp. 152–160, 2010.
- [5] D. K. Das, M. S. Islam, C. B. Dutta, M. M. Hassan, and S. S. Hossen, “Is there any demand for improved cooking stoves? Evidence from Bangladesh,” *Journal of Environmental Management*, vol. 298, article 113412, 2021.
- [6] S. Jewitt, P. Atagher, and M. Clifford, ““We cannot stop cooking”: Stove stacking, seasonality and the risky practices of household cookstove transitions in Nigeria,” *Energy Research & Social Science*, vol. 61, article 101340, 2020.
- [7] O. Masera, R. Bailis, A. Ghilardi et al., “Environmental Burden of Traditional Bioenergy Use,” *Article in Annual Review of Environment and Resources*, vol. 40, no. 1, pp. 121–150, 2015.
- [8] D. Zhao, M. Yan, L. Guo et al., “Cooking stoves and risk of congenital heart disease in Northwest China: a case-control study,” *Science of The Total Environment*, vol. 816, article 151564, 2022.
- [9] M. Aramesh, M. Ghalebani, A. Kasaeian et al., “A review of recent advances in solar cooking technology,” *Renewable Energy*, vol. 140, pp. 419–435, 2019.



- [10] Y. Zhao, L. Liu, P. Tao et al., "Review of effluents and health effects of cooking and the performance of kitchen ventilation," *Aerosol and Air Quality Research*, vol. 19, no. 8, pp. 1937–1959, 2019.
- [11] U. C. Arunachala and A. Kundapur, "Cost-effective solar cookers: a global review," *Solar Energy*, vol. 207, pp. 903–916, 2020.
- [12] A. Weldu, L. Zhao, S. Deng et al., "Performance evaluation on solar box cooker with reflector tracking at optimal angle under Bahir Dar climate," *Solar Energy*, vol. 180, pp. 664–677, 2019.
- [13] O. A. Jaramillo, G. Huelsz, G. Hernández-Luna, J. A. del Río, R. Acosta, and L. G. Arriaga, "Solar oven for intertropical zones: optogeometrical design," *Energy Conversion and Management*, vol. 48, no. 10, pp. 2649–2656, 2007.
- [14] A. Regattieri, F. Piana, M. Bortolini, M. Gamberi, and E. Ferrari, "Innovative portable solar cooker using the packaging waste of humanitarian supplies," *Renewable and Sustainable Energy Reviews*, vol. 57, pp. 319–326, 2016.
- [15] A. Herez, M. Ramadan, and M. Khaled, "Review on solar cooker systems: economic and environmental study for different Lebanese scenarios," *Renewable and Sustainable Energy Reviews*, vol. 81, pp. 421–432, 2018.
- [16] L. Nkhonjera, T. Bello-Ochende, G. John, and C. K. King'ondo, "A review of thermal energy storage designs, heat storage materials and cooking performance of solar cookers with heat storage," *Renewable and Sustainable Energy Reviews*, vol. 75, pp. 157–167, 2017.
- [17] R. Farhadi and M. Taki, "The energy gain reduction due to shadow inside a flat-plate solar collector," *Renewable Energy*, vol. 147, pp. 730–740, 2020.
- [18] F. Sosa-Montemayor, O. A. Jaramillo, and J. A. del Río, "Thermodynamic analysis of a solar coffee maker," *Energy Conversion and Management*, vol. 50, no. 9, pp. 2407–2412, 2009.
- [19] O. K. Singh, "Development of a solar cooking system suitable for indoor cooking and its exergy and enviroeconomic analyses," *Solar Energy*, vol. 217, pp. 223–234, 2021.
- [20] J. Yu, Y. M. Tang, K. Y. Chau, R. Nazar, S. Ali, and W. Iqbal, "Role of solar-based renewable energy in mitigating CO<sub>2</sub> emissions: evidence from quantile-on-quantile estimation," *Renewable Energy*, vol. 182, pp. 216–226, 2022.
- [21] S. Indora and T. C. Kandpal, "Institutional cooking with solar energy: a review," *Renewable and Sustainable Energy Reviews*, vol. 84, pp. 131–154, 2018.
- [22] M. S. Nazir, A. J. Mahdi, M. Bilal, H. M. Sohail, N. Ali, and H. M. Iqbal, "Environmental impact and pollution-related challenges of renewable wind energy paradigm – a review," *Science of the Total Environment*, vol. 683, pp. 436–444, 2019.
- [23] A. A. Omara, A. A. Abuelnuor, H. A. Mohammed, D. Habibi, and O. Younis, "Improving solar cooker performance using phase change materials: a comprehensive review," *Solar Energy*, vol. 207, pp. 539–563, 2020.
- [24] A. Saxena and N. Agarwal, "Performance characteristics of a new hybrid solar cooker with air duct," *Solar Energy*, vol. 159, pp. 628–637, 2018.
- [25] A. Saxena, S. K. Joshi, P. Gupta et al., "An experimental comparative analysis of the appropriateness of different sensible heat storage materials for solar cooking," *Journal of Energy Storage*, vol. 61, article 106761, 2023.
- [26] T. K. Gawande and D. S. Ingole, "Comparative study of heat storage and transfer system for solar cooking," *SN Applied Sciences*, vol. 1, no. 12, 2019.
- [27] Food Standards Agency, *Cooking your food*, Food Standards Agency, 2018.
- [28] S. Elshahat, J. V. Woodside, and M. C. McKinley, "Meat thermometer usage amongst European and North American consumers: a scoping review," *Food Control*, vol. 106, article 106692, 2019.
- [29] C. R. Ruivo, G. Coccia, G. Di Nicola, A. Carrillo-Andrés, and X. Apaolaza-Pagoaga, "Standardised power of solar cookers with a linear performance curve following the Hottel-Whillier-Bliss formulation," *Renewable Energy*, vol. 200, pp. 1202–1210, 2022.
- [30] S. Verma, S. Banerjee, and R. Das, "A fully analytical model of a box solar cooker with sensible thermal storage," *Solar Energy*, vol. 233, pp. 531–542, 2022.
- [31] G. Coccia, G. Di Nicola, M. Pierantozzi, S. Tomassetti, and A. Aquilanti, "Design, manufacturing, and test of a high concentration ratio solar box cooker with multiple reflectors," *Solar Energy*, vol. 155, pp. 781–792, 2017.
- [32] S. Joshi and A. Jani, "Design, development and testing of a small scale hybrid solar cooker," *Solar Energy*, vol. 122, pp. 148–155, 2015.
- [33] A. A. Sagade, S. Samdarshi, and P. Panja, "Experimental determination of effective concentration ratio for solar box cookers using thermal tests," *Solar Energy*, vol. 159, pp. 984–991, 2018.
- [34] A. A. Sagade, S. Samdarshi, and P. S. Panja, "Enabling rating of intermediate temperature solar cookers using different working fluids as test loads and its validation through a design change," *Solar Energy*, vol. 171, pp. 354–365, 2018.
- [35] P. E. D. Augusto and M. Cristianini, "Determining the convective heat transfer coefficient (h) in thermal process of foods," *International Journal of Food Engineering*, vol. 7, no. 4, 2011.
- [36] B. P. Mahanta, P. K. Bora, P. Kemprai, G. Borah, M. Lal, and S. Haldar, "Thermolabile essential oils, aromas and flavours: degradation pathways, effect of thermal processing and alteration of sensory quality," *Food Research International*, vol. 145, article 110404, 2021.
- [37] A. Mawire, K. Lentswe, P. Owusu et al., "Performance comparison of two solar cooking storage pots combined with wonderbag slow cookers for off-sunshine cooking," *Solar Energy*, vol. 208, pp. 1166–1180, 2020.
- [38] M. Pasrija and D. Punia, "Effect of pressure and solar cooking on phytic acid and polyphenol content of cowpeas," *Nutrition & Food Science*, vol. 30, no. 3, pp. 133–137, 2000.
- [39] S. Tapia-Salinas, J. del Río, and O. Jaramillo, *Mx 340215b patent food solar cooker with electric backing*, IMPI, 2006.
- [40] J. L. Ayala Hernández, S. Demesa Udave, M. A. Delgado Yoshino, S. Tapia Salinas, and J. A. del Río Portilla, *El Sabor de la Comida Solar*, Correo del Maestro, 2009.
- [41] J. A. del Río, S. Tapia-Salinas, and O. A. Jaramillo, "Solar cookers," *Revista Digital Universitaria*, vol. 11, pp. 1–11, 2010.
- [42] J. C. Castro Domínguez, *Evaluación de un Cocedor Solar Doméstico, [M.S. thesis]*, Universidad Nacional Autónoma de México, México, 2013, <https://repositorio.unam.mx/contenidos/evaluacion-de-un-cocedor-solardomestico-124372>.
- [43] S. Tapia-Salinas, *Cocedor solar con respaldo electrico, [M.S. thesis]*, Universidad Nacional Autónoma de México, México, 2005.
- [44] J. A. del Río, S. Tapia-Salinas, and O. A. Jaramillo, *Mx 2008006472a patent solar tracking semi-circular device*, IMPI, 2008.



- [45] AOAC International, *Official Methods of Analysis of AOAC International*, AOAC INTERNATIONAL, 2012.
- [46] Z. M. Mendoza and P. H. Borges, "Análisis colorimétrico del extracto acuoso de hojas de TECA1," *Revista Árvore*, vol. 39, no. 5, pp. 953–961, 2015.
- [47] A. Patras, "Stability and colour evaluation of red cabbage waste hydroethanolic extract in presence of different food additives or ingredients," *Food Chemistry*, vol. 275, pp. 539–548, 2019.
- [48] P. Malo and E. Urquhart, "Fermented foods: use of starter cultures," in *Encyclopedia of Food and Health*, B. Caballero, P. M. Finglas, and F. Toldrá, Eds., pp. 681–685, Academic Press, Oxford, 2016.
- [49] D. C. Montgomery, *Design and analysis of experiments*, John-Wiley & Sons, Inc., Hoboken, NJ, 10th edition, 2020, <https://www.wiley.com/en-us/Design+and+Analysis+of+Experiments%2C+10th+Edition-p-9781119492443>.
- [50] S. Badui Dergal, *Química de los alimentos*, Perason Education S. A, sixth edition, 2019.
- [51] L. Costeña, "Tamal de elote," 2018, <https://www.lacostena.com.mx/en/products/corn-tamale/>.
- [52] L. M. M. Market, "Tamal de elote," 2018, <https://www.lamichoacanameatmarket.com/tamal-de-elote/>.
- [53] W. Frazier and D. Westhoff, *Microbiología de los alimentos*, Editorial Acribia, S.A., fourth edition, 1993.
- [54] S. P. Betancourt Botero, G. A. Bolívar Escobar, and C. Ramírez Toro, "Fermentación de maíz de alta calidad proteica con *Lactobacillus plantarum* (CPQBA 087-11 DRM) aislado en Colombia de masas tradicionales fermentadas," *Revista Argentina de Microbiología*, vol. 45, no. 4, pp. 282-283, 2013.
- [55] W. Huang, D. Fan, W. Li, and Y. Meng, "Rapid evaluation of milk acidity and identification of milk adulteration by Raman spectroscopy combined with chemometrics analysis," *Vibrational Spectroscopy*, vol. 123, article 103440, 2022.